Volume No.03, Special Issue No. 02, February 2015 ISSN (online): 2348 – 7550

EFFECT OF TEMPERATURE ON DENSIFICATION OF Y_2O_3:SiO_2 POWDER

Rachna Ahlawat

Department of Physics, Materials Science Lab., Ch. Devi Lal University, Sirsa, Haryana (India)

ABSTRACT

Y_2O_3:SiO_2 powder was synthesized by a sol gel method, using hydrous yttrium nitrate and hydrous silicon oxide as precursors and HCl as a catalyst. The dried samples were annealed at different temperature in air using multi step scheme with a final stage of about 900°C for 6.0 hours. The samples of Y_2O_3:SiO_2 powder were obtained with high densification and well defined size and shape. Structural changes of the nano powder were investigated by XRD and TEM. Activation energy and micro stain were also calculated for the prepared samples. Almost fully dense spherical yttria nanopowder has been demonstrated with an average grain size distribution of 30 nm which are uniformly dispersed with in silica matrix.

Keywords: Nanopowder, Sol-gel Technique, Multistep annealing, XRD, TEM.

I. INTRODUCTION

For the development of powder technology, in particular, demands as a building blocks due to the increase in structural and compositional complexity so that they can be produced with ease, in abundance, at low cost and low temperature. Nano powders containing nanocrystalline rare-earth oxides (R_2O_3) and silica have been investigated widely due to their use in many fields [1-3]. The application of nanocrystalline materials as a powder feedstock for thermal spraying has been facilitated with a wide range of powder sources such as vapor condensation, combustion synthesis, thermo chemical synthesis, co-precipitation and mechanical alloying/milling and sol-gel process, etc [4-5]. Among the various powder sources, sol-gel process has the advantage of lower temperature, possibility of making a finely dispersed powder, easy to make and at low cost. Cannas et al. [6] used sol-gel method to prepare Y_2O_3:SiO_2, after thermal treatment of samples at moderate temperature T ~ 900°C (0.5 h) and high temperature 1300°C (0.5 h) in air. They found Y_2O_3:SiO_2 as an amorphous when it was sintered at moderate temperature. In another case, Xiaoyi et al. [7] used co-precipitation technique to synthesize Y_2O_3:SiO_2 samples. The prepared powder samples were thermally treated around T~800°C and their structural characterizations were demonstrated. In order to prepare powder of nanocomposites, two- and three- step sintering process has been used by many researchers [8-9].

In the light of above discussion, we have first time shown monitoring of shape, size and densification of Y_2O_3:SiO_2 powder using multi-step annealing. Using four step annealing scheme, quasi-spherical Y_2O_3 nanocrystallites has been obtained in SiO_2. In addition, we have also shown that size and crystallinity of Y_2O_3 nanocrystallites increase almost linearly with increasing the annealing temperature.

II. EXPERIMENTAL

2.1 Sample Preparation

Using sol-gel technique, the samples of Y_2O_3:SiO_2 powder was prepared. The complete description of the synthesis method has been given in our earlier publication [10]. In forthcoming subsections dried sample is named as-prepared (a) and annealed samples are designated as: (b), (c), (d) and (e) according to their respective annealing schemes as shown in the Fig. 1.

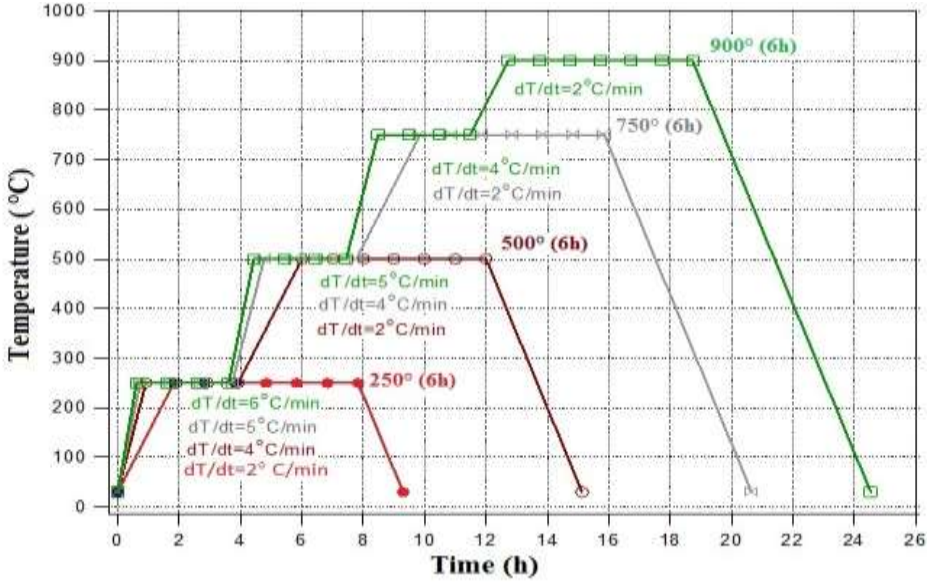

Figure 1: Schematic Diagram of Annealing Scheme

2.2 Characterizations

As-prepared and annealed samples were characterized by an X'pert Pro X-Ray Diffractometer with Cu-$k_{\alpha 1}$ radiation in the range of 5^o-80^o in steps of 0.017^o (40mA, 45KV) for the determination of crystalline structure of nanocomposites. Shapes, sizes and morphologies were further confirmed by HRTEM Hitachi 4500 micrograph. The samples were prepared for TEM imaging by drying aforesaid samples on a copper grid that was coated with a thin layer of carbon then analyzed using a Hitachi 4500 micrograph.

III. RESULTS AND DISCUSSION

3.1. XRD

XRD pattern of as-prepared sample (a) and the annealed samples at different conditions have been shown in the Fig. 2. The diffraction pattern of as-prepared sample (a) depicts two very strong and sharp diffraction lines centered at 2θ ~ 13.96°, 25.65° and a series of weak peaks lying between 30° to 70°. The sharp lines could be ascribed to the characteristic diffraction of yttrium nitrate hydrate (JCPDS card no. 84-2195) and silicon oxide hydrate (JCPDS card no. 82-1179). These sharp lines of dried-sample signify bulk behavior of hydrous precursor's nuclei and also suggest that the precursors have not decomposed. The XRD pattern of the sample (b) reveals that the precursor yttrium nitrate hydrate was almost decomposed which is confirmed by disappearance of its characteristics peak at 2θ ~ 13.96°. However, no significant change is evident in the characteristics peak of the precursor silicon oxide hydrate which entails that precursor was still not decomposed.

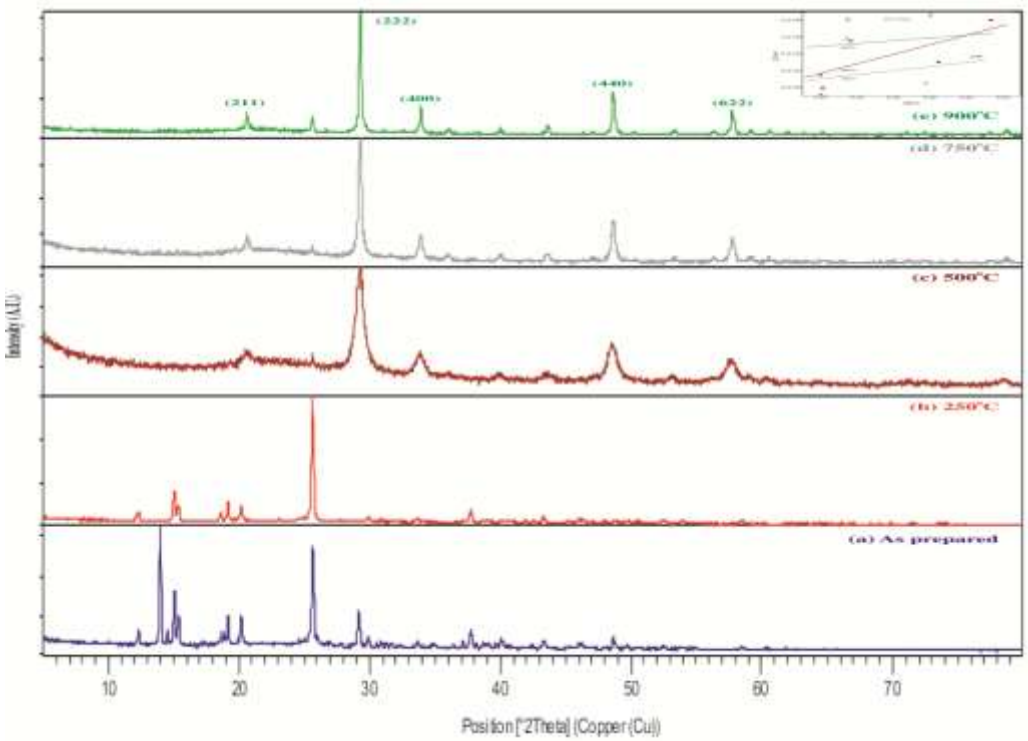

Figure 2: XRD Patterns Of As-Prepared and Annealed Samples of Y_2O_3:Sio_2 Powder

However, in diffraction pattern of sample (c), the characteristic peak of the precursor silicon oxide hydrate disappeared which implies that this precursor has been decomposed and interfacial interaction has also been started in the sample. A strong but slightly broad new peak appeared at 2θ ~ 29.25° with some weak new peaks at 2θ ~ 20.62°, 33.85°, 48.58°, 57.77° in the diffraction pattern. The occurrence of these new peaks infers the development of a new polycrystalline phase in the sample. In order to identify structure of the polycrystalline phase, "Check cell" code was run and found that plane corresponding to diffraction peaks at 2θ~ 20.62°, 33.85°, 48.58°, 57.77° could be assigned to Miller indices (211), (400), (440), (622), respectively of the cubic Y_2O_3 structure having lattice parameter a = 10.56 Å and space group Ia3 (T_h^7) [11]. Moreover, Miller indices were also confirmed by comparing the obtained Check cell data with the JCPDS card no. 41-1105. On further inspection of sample (c), a hump between 2θ~20^o-26^o along with a small peak centered at 2θ ~ 25.64° is clearly evident in the Fig. 2 for strengthening of vitreous silica. Furthermore, temperature was raised up to 750°C (6.0 h) by three-step annealing to examine structural changes and crystallinity of cubic Y_2O_3:SiO_2 polycrystalline powder. A significant increase in intensity and sharpness of the characteristic peaks of Y_2O_3 (JCPDS card no. 84-2195) indicates the increase in its crystallinity and size. By minute observations, one may notice a crystalline peak (2θ ~ 25.62°) emerged over the vitreous silica residual background, which can be attributed to characteristic lines of the quartz. These results give confidence that annealing conditions of sample (d) is more or less sufficient to obtain cubic Y_2O_3 nanocrystallites with a well-defined size in crystalline silica matrix. On the other hand, literature reveals a conventional heat treatment for dried Y_2O_3:SiO_2 sample at T ~ 900°C for (0.5 h) and yielded amorphous Y_2O_3:SiO_2 composites [6]. We have annealed the sample (e) by four-step annealing in which final stage annealing was done at 900°C for 6.0 hrs and found that the intensity and sharpness of the characteristics peaks have increased significantly, which infers further improvement of crystallinity and size of Y_2O_3. The XRD results suggest that the crytallinity and densification of Y_2O_3 nanocrystallites in crystalline SiO_2 matrix can be tailored by varying ramp rates and annealing temperatures.

3.1.1 Crystallite Size and Micro-Strain Calculations

The micro-strain and crystallite size produces peak broadening in the diffractogram. The crystallite size and the strain effect can be differentiated in the diffractogram. Both effects are independent and can be distinguished by the W-H plot. The W-H equation is:

$$\beta_{hkl}Cos(\theta)_{hkl}=K\lambda/D+2\varepsilon Sin(\theta)_{hkl} \quad \ldots(1)$$

where K is the shape factor which is 0.9 for uniform small size crystals, λ is the wavelength of X-ray, θ_{hkl} is the Bragg angle, ε is the micro-strain and *D* is average crystallite size measured in a direction perpendicular to the surface of the specimen. The graph is plotted between Sin $(\theta)_{hkl}$ and β_{hkl} Cos$(\theta)_{hkl}$ as shown in the inset of Fig. 2. From this graph, value of the micro-strain is estimated using slope of the line and found 1.41×10^{-3}, 1.19×10^{-3} and 1.05×10^{-3}, respectively for samples (c), (d) and (e). The nano crystallite size has also been calculated ~ 13 nm, 21 nm and 35 nm from the intersection along the vertical axis. In the Fig. 3, micro-strain *(right vertical axis)* versus 1/T is plotted. It was noticed that micro-strain reduces gradually with increasing annealing temperature. Moreover, influence of micro strain (ε) on peak broadening is negligibly small. Under these considerations, Williamson-Hall relation reduces to a well known Debye-Scherer's equation:

$$D=K\lambda/\beta Cos\theta \quad \ldots (2)$$

The average crystallite size (*D*) of cubic Y_2O_3 was also estimated using Debye-Scherer's equation and found 10 nm, 20 nm and 33 nm, respectively for samples (c), (d) and (e). The average crystallite size estimated by the Williamson-Hall and Debye-Scherer's equation is found almost equal because influence of micro-strain in the peak broadening was very weak due to multi-step annealing.

3.1.2 Activation Energy

Crystallite growth is a crucial aspect of thermal stability of the nanocrystalline solids. Nanocrystalline materials are thermodynamically unstable due to the presence of a large fraction of interface boundaries. There is a strong tendency for nanocrystalline materials to convert to conventional coarser grain materials with fewer interfaces. Therefore, stabilization of the nanocrystalline grain structure is of critical importance.

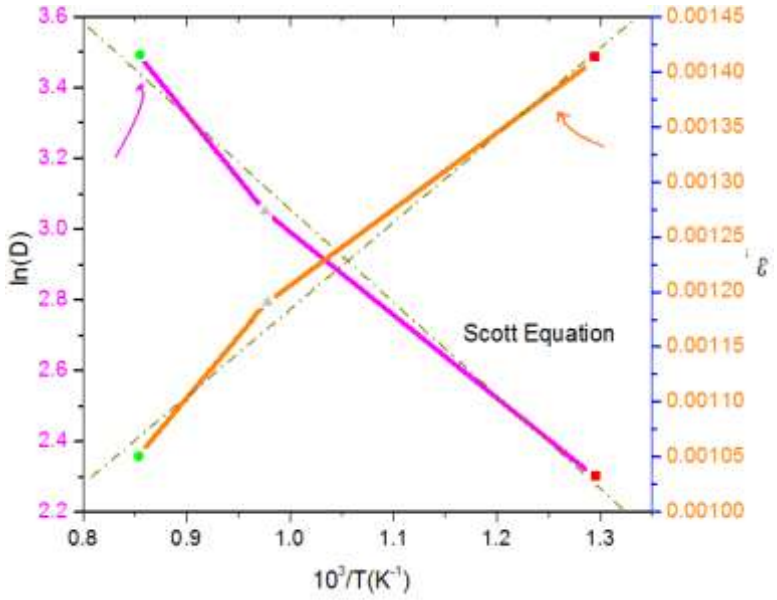

Figure 3: Variation Of Crystalline Size (Left Verticle Axis) And Micro-Strain (Right Verticle Axis) Vs. 1/T. Dotted Lines Repersent Fitting Of Data

If the growth rate of crystallite from thermal treatment is known, then using Scott relation: $D = C \exp(-E/RT)$, where C is a constant, R is the ideal gas constant; one may estimate activation energy (E) for the grain growth [12]. The activation energy value is obtained E = 25.6 KJ/mol from the slope of the straight line of plot between ln (*D*) versus 1/T as shown in the Fig. 3. It has been observed that activation energy of Y_2O_3 nanopowder is found nearly 5 times smaller than the activation energy of Y_2O_3 bulk powder [13]. In the Fig. 3, almost linear relationship between crystallites size *(left vertical axis)* and inverse of final stage annealing temperature suggests crystallite growth primarily by means of an interfacial reaction in Y_2O_3:SiO_2 composite [11]. This result suggests that crystallites size of cubic Y_2O_3 nano powder almost increases linearly with increasing annealing temperature.

3.3 Transmission Electron Microscopy

The transmission electron microscopy (TEM) of as-prepared (a) and annealed powder samples (c), (d), (e), are shown in the Fig. 4. The selected-area electron-diffraction (SAED) pattern of the individual nanoparticles was obtained (inset) to evaluate their crystalline nature.

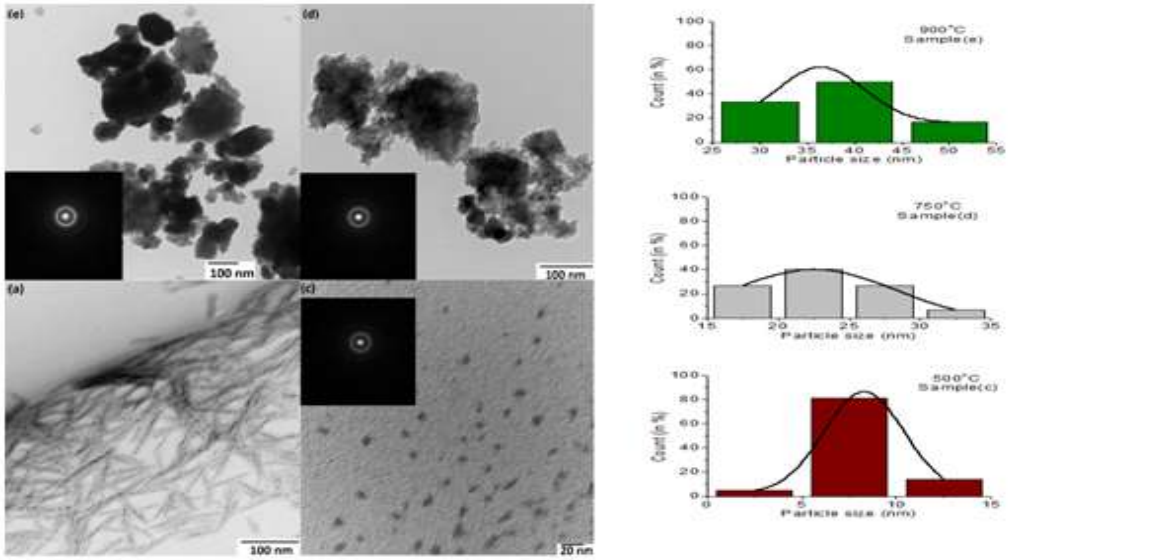

Figure 4: TEM Micrographs Of Samples: (A), (C), (D) And (E). Inset Show Slected-Area Electron Diffraction

(SAED) patter of the micrograph. Particle size distribution for (c), (d) and (e) samples has also been shown.

As expected, micrograph of samples (a & b) shows typical chain-like structure of acidic gel of precursors and confirms the results of XRD of this sample. The TEM image of sample (c) shows non-agglomerated yttria nanocrystallites of quasi-spherical shape having size ranges 8-10 nm and grain size distribution shows that nano Y_2O_3 have narrow grain size distribution in the silica matrix as shown in the Fig 4. Corresponding ring pattern of this sample indicates a weak polycrystalline nature of the sample and this result suggests that the FTIR and XRD results are in close agreement with one another.

The TEM micrograph of sample (d) illustrates coalesces of yttria nanocrystallite and resulted in bigger size (15-30 nm); among them 40 % crystallites are having their size 25-30 nm as shown in the particle size distribution. The SAED pattern of this sample verifies that the synthesized nanocrystallites have better polycrystalline nature than the sample (c). In the case of sample (e), annealing was demonstrated by a four-step program. The TEM micrograph of sample (e) depicts a densified and almost fully crystalline yttria nanopowder and its size has been increased significantly. Histogram as shown in the Fig. 4 reveals that nearly 50 % crystallites are having size

ranges 35-45 nm and the sample (e) has comparatively wider grain size distribution than that of sample (c) annealed via two-step process.

Hence it may be concluded from the TEM micrographs that crystallites growth of Y_2O_3 in crystalline SiO_2 proceeded by grain boundary diffusion mechanism while densification occurs due to grain boundary migration.

IV. CONCLUSION

Using sol-gel method Y_2O_3:SiO_2 nanocomposite was successfully obtained by multi-step annealing process. In single-step annealing, at low temperature T~ 250°C, yttrium nitrate hydrate was decomposed, while in two-step, silicon oxide hydrate was decomposed and interfacial solid-state interaction resulted in formation of Y_2O_3:SiO_2 polycrystalline powder. The crystallites were found to be 5-10 nm with quasi-spherical shape and homogenously dispersed with quite narrow size distribution in silica matrix. In three-step annealing, a significant increase in intensity and sharpness of Y_2O_3 characteristic peaks indicates increase in its crystallinity, densification and size. Four-step annealing produced almost fully crystallized with less micro-strain, stable, pure and densified, cubic-yttria nanopowder in crystalline silica matrix.

REFERENCES

[1] F. Branda in: Advances in nanocomposite: Synthesis, Characterization and Industrial applications Eds. B.S.R. Reddy, Ch 14, 2011.

[2] A. Iyer, J.K.M. Garofano, J. Reutenaur, S.L. Suib, M. Aindow, M. Gell, E. H M. Jordan, A. Gell, Sucrose-Mediated Sol–Gel Technique for the Synthesis of MgO–Y_2O_3 Nanocomposites, J. Am. Ceram. Soc. 96 (2013) 346-350.

[3] K. Ariga, J.P. Hill, M.V. Lee, A. Vinu, R. Charvet, S. Acharya, Challenges and breakthroughs in recent research on self-assembly, Sci. Technol. Adv. Mater. 9 (2008) 014109.

[4] S. Duhan, P. Aghamkar, Bhajan Lal, Effect of thermal annealing on Nd_2O_3-doped silica powder prepared by the solgel process, J. Alloys Compd. 474 (2009) 301-305.

[5] P. Aghamkar, S. Duhan, M. Singh, N. Kishore, P.K. Sen, Effect of thermal annealing on Nd_2O_3-doped silica powder prepared by the solgel process, J. of Sol-Gel Sci. and Tech. 46 (2008) 17-22.

[6] C. Cannas, M. Casu, A. Lai, A. Musinu, and G. Piccaluga, Study of the nanoparticle/matrix interactions in Y_2O_3–SiO_2 samples, Phys. Chem. Chem. Phys. 4 (2002) 2286-2292.

[7] S. Xiaoyi and Z. Yuchun, Preparation and optical properties of Y_2O_3/SiO_2 powder, Rare Met. 30 (2011) 33-38.

[8] X-H Wang, I-W Chen, Synthesis of nanocomposites, Nanomaterials Handbook, Eds. Y. Gogosti, CRC Press, 2006, Ch. 12

[9] M. Dagfinn, S.Crina, W. Ivar, A.C. Hoffmann, Sintering of 4YSZ (ZrO_2^{+4} mol% Y_2O_3) nanoceramics for solid oxide fuel cells (SOFCs), their structure and ionic conductivity, J. Eur. Ceram. Soc. 29 (2009) 2537-2547.

[10] Rachna and P. Aghamkar, Optical Materials, 36 (2013) 337.

[11] R.G. Haire, L. Eyring, Comparisons of the Binary Oxides, Handbook on the Physics and Chemistry of Rare Earths, Vol. 18, ed. by K. A. Gschneidner, Jr., L. Eyring, G R. Choppin, G. R. Lander (North-Holland, Amsterdam, 1994), Chap. 12.

[12] M.G. Scott, Amorphous Metallic Alloys, Butterworth, London, (1983), p.151.

[13] L.G. Jacobsohn, M.W. Blair, S.C. Tornga, L.O. Brown, B.L. Bennett, R.E. Muenchausen, Y_2O_3:Bi nanophosphor: Solution combustion synthesis, structure, and luminescence, J. Appl. Phys. 104 (2008) 124303-10.